

Production and polarization of the Λ_c^+ and the charm of the proton *

J. C. Anjos **G. Herrera** [†] **J. Magnin** [‡]
F.R.A. Simão

Centro Brasileiro de Pesquisas Físicas
 Rua Dr. Xavier Sigaud 150
 22290-180, Rio de Janeiro, Brazil

PACS 13.60.Rj (Baryon production)
 13.87.Fh (Fragmentation into hadrons)
 14.20.Lq (Charmed baryons)

Abstract

We propose a two-component model involving the parton fusion mechanism and recombination of a ud valence diquark with a sea c -quark of the incident proton to describe Λ_c^+ inclusive production in pp collisions. We also study the polarization of the produced Λ_c^+ in the framework of the Thomas Precession Model for polarization. We show that a measurement of the Λ_c polarization is a sensitive test of its production mechanism. In particular the intrinsic charm model predicts a positive polarization for the Λ_c within the framework of the Thomas Precession Model, while according to the model presented here the Λ_c polarization should be negative. The measurement of the Λ_c polarization provides a close examination of intrinsic charm Fock states in the proton and gives interesting information about the hadroproduction of charm.

*This work was partially supported by Centro Latino Americano de Física (CLAF).

[†]Permanent address: Centro de Investigación y de Estudios Avanzados, Apdo. Postal 14 740, México 07000, DF, Mexico. e-mail: gherrera@fis.cinvestav.mx

[‡]e-mail: jmagnin@lafex.cbpf.br

1 Introduction

The production mechanism of hadrons containing heavy quarks is not well understood. Although the fusion reactions $gg \rightarrow Q\bar{Q}$ and $q\bar{q} \rightarrow Q\bar{Q}$ are supposed to be the dominant processes, they fail to explain important features in hadro-production like the leading particle effects observed in D^\pm produced in π^-p collisions [1], Λ_c^+ produced in pp interactions [2, 3, 4] and others baryons containing heavy quarks [5], the J/Ψ cross section at large x_F observed in πp collisions [6], etc.

The above mentioned effects have been explained using a two-component model [7] which consists of the parton fusion mechanism, calculable in perturbative QCD, plus the coalescence of intrinsic charm [8].

Here we present an alternative mechanism, namely the conventional recombination of valence spectator quarks with a c -quark present in the sea of the initial hadron.

We show that this mechanism can explain the production enhancement at large x_F observed in charmed hadron production in hadronic interactions.

We describe the Λ_c^+ production in pp interactions with a two-component model consisting of the recombination of a diquark ud with a c -quark from the sea of the incident proton plus the usual parton fusion and fragmentation mechanism. We compare the obtained results with those of the intrinsic charm two-component model and with experimental data.

We also study the polarization of Λ_c^+ using the Thomas Precession Model (TPM) [9] for both the intrinsic charm model and the conventional recombination two component model presented here. We show that the polarization prediction of this two models is totally different and conclude that a measurement of the polarization can be an important source of information to uncover the processes behind heavy hadron production.

2 Λ_c^+ production in p-p collisions

In this section we give the prediction of the two component model for the cross section as a function of x_F . In section 2.1 we show the calculation of parton fusion and fragmentation and in section 2.2 the recombination picture is presented.

2.1 Λ_c^+ production *via* parton fusion

In the parton fusion mechanism the Λ_c^+ is produced *via* the subprocesses $q\bar{q}(gg) \rightarrow c\bar{c}$ with the subsequent fragmentation of the c quark. The inclusive x_F distribution of the Λ_c^+ in pp collisions is given by [10, 11]

$$\frac{d\sigma^{pf}}{dx_F} = \frac{1}{2}\sqrt{s} \int H_{ab}(x_a, x_b, Q^2) \frac{1}{E} \frac{D_{\Lambda_c/c}(z)}{z} dz dp_T^2 dy, \quad (1)$$

where

$$\begin{aligned} H_{ab}(x_a, x_b, Q^2) = & \Sigma_{a,b} \left(q_a(x_a, Q^2) \bar{q}_b(x_b, Q^2) \right. \\ & + \bar{q}_a(x_a, Q^2) q_b(x_b, Q^2) \left. \right) \frac{d\hat{\sigma}}{d\hat{t}} \Big|_{q\bar{q}} \\ & + g_a(x_a, Q^2) g_b(x_b, Q^2) \frac{d\hat{\sigma}}{d\hat{t}} \Big|_{gg}, \end{aligned} \quad (2)$$

with x_a and x_b being the parton momentum fractions, $q(x, Q^2)$ and $g(x, Q^2)$ the quark and gluon distributions in the proton, E the energy of the produced c -quark and $D_{\Lambda_c/c}(z)$ the fragmentation function measured in e^+e^- interactions. In eq. 1, p_T^2 is the squared transverse momentum of the produced c -quark, y is the rapidity of the \bar{c} quark and $z = x_F/x_c$ is the momentum fraction of the charm quark carried by the Λ_c^+ . The sum in eq. 2 runs over $a, b = u, \bar{u}, d, \bar{d}, s, \bar{s}$.

We use the LO results for the elementary cross-sections $\frac{d\hat{\sigma}}{d\hat{t}} \Big|_{q\bar{q}}$ and $\frac{d\hat{\sigma}}{d\hat{t}} \Big|_{gg}$ [10].

$$\frac{d\hat{\sigma}}{d\hat{t}} \Big|_{q\bar{q}} = \frac{\pi\alpha_s^2(Q^2)}{9\hat{m}_c^4} \frac{\cosh(\Delta y) + m_c^2/\hat{m}_c^2}{[1 + \cosh(\Delta y)]^3} \quad (3)$$

$$\frac{d\hat{\sigma}}{d\hat{t}} \Big|_{gg} = \frac{\pi\alpha_s^2(Q^2)}{96\hat{m}_c^4} \frac{8\cosh(\Delta y) - 1}{[1 + \cosh(\Delta y)]^3} \left[\cosh(\Delta y) + \frac{2m_c^2}{\hat{m}_c^2} + \frac{2m_c^4}{\hat{m}_c^4} \right], \quad (4)$$

where Δy is the rapidity gap between the produced c and \bar{c} quarks and $\hat{m}_c^2 = m_c^2 + p_T^2$. The Feynman diagrams involved in the calculation of eqs. 3 and 4 are shown in fig. 1.

In order to be consistent with the LO calculation of the elementary cross sections, we use the GRV-LO parton distribution functions [12]. A global factor $K \sim 2 - 3$ in eq. 1 takes into account NLO contributions [13].

We take $m_c = 1.5 \text{ GeV}$ for the c -quark mass and fix the scale of the interaction at $Q^2 = 2m_c^2$ [10]. Following [7], we use two fragmentation functions

to describe the charm quark fragmentation;

$$D_{\Lambda_c/c}(z) = \delta(1 - z) \quad (5)$$

and the Peterson fragmentation function [14]

$$D_{\Lambda_c/c}(z) = \frac{N}{z [1 - 1/z - \epsilon_c/(1 - z)]^2} \quad (6)$$

with $\epsilon_c = 0.06$ and the normalization defined by $\sum_H \int D_{H/c}(z) dz = 1$.

2.2 Λ_c^+ production *via* recombination

The production of leading mesons at low p_T was described by recombination of quarks long time ago [15]. The method introduced by Das and Hwa for mesons was extended by Ranft [16] to describe single particle distributions of leading baryons in pp collisions. Recently a more sophisticated version of the recombination model using the concept of valons [17] has been used to study D^\pm asymmetries in π^-p interactions [18].

In recombination models it is assumed that the outgoing leading hadron is produced in the beam fragmentation region through the recombination of the maximum number of valence- and the minimum number of sea- quarks. Thus Λ_c^+ 's produced in pp collisions are formed by an u and a d valence quarks and a c sea quark from the incident proton. Contributions involving the recombination of more than one sea flavor are neglected.

The invariant inclusive x_F distribution for leading baryons is given by

$$\frac{2E}{\sigma\sqrt{s}} \frac{d\sigma^{rec}}{dx_F} = \int_0^{x_F} \frac{dx_1}{x_1} \frac{dx_2}{x_2} \frac{dx_3}{x_3} F_3(x_1, x_2, x_3) R_3(x_1, x_2, x_3, x_F), \quad (7)$$

where x_i , $i = 1, 2, 3$, is the momentum fraction of the i^{th} quark, $F_3(x_1, x_2, x_3)$ is the three-quark distribution function in the incident hadron and $R_3(x_1, x_2, x_3, x_F)$ is the three-quark recombination function.

The Λ_c^+ production by recombination is shown in schematic form in fig. 2.

We use a parametrization containing explicitly the single quark distributions for the three-quark distribution function

$$F_3(x_1, x_2, x_3) = \beta F_{u,val}(x_1) F_{d,val}(x_2) F_{c,sea}(x_3) (1 - x_1 - x_2 - x_3)^\gamma \quad (8)$$

with $F_q(x_i) = x_i q(x_i)$ and F_u normalized to one valence u quark. The parameters β and γ are constants fixed by the consistency condition

$$F_q(x_i) = \int_0^{1-x_i} dx_j \int_0^{1-x_i-x_j} dx_k F_3(x_1, x_2, x_3),$$

$$i, j, k = 1, 2, 3 \quad (9)$$

for the valence quarks of the incoming protons as in ref. [16].

We use the GRV-LO parametrization for the single quark distributions in eqs. 8 and 9. It must be noted that since the GRV-LO distributions are functions of x and Q^2 , our $F_3(x_1, x_2, x_3)$ also depends on Q^2 .

In contrast with the parton fusion calculation, in which the scale Q^2 of the interaction is fixed at the vertices of the appropriated Feynman diagrams, in recombination there is not clear way to fix the value of the parameter Q^2 , which in this case is not properly a scale parameter and should be used to give the content of the recombining quarks in the initial hadron.

Since the charm content in the proton sea increases rapidly for Q^2 growing from m_c^2 to Q^2 of the order of some m_c^2 's when it becomes approximately constant, we take $Q^2 = 4m_c^2$, a conservative value, but sufficiently far from the charm threshold in order to avoid a highly depressed charm sea which surely does not represent the real charm content of the proton. At this value of Q^2 we found that the condition of eq. 9 is fulfilled approximately with $\gamma = -0.1$ and $\beta = 75$. We have verified that the recombination cross section does not change appreciably at higher values of Q^2 .

The value of Q^2 in recombination could be different from the scale of the interaction in parton fusion. In fact, in the later the scale of the interaction should be chosen to be of the order of the hard momentum scale while in recombination, the value of Q^2 must be chosen in such a way that the true content of quarks be present to form the outgoing hadron, allowing in this way a more higher value of this parameter.

For the three-quark recombination function for Λ_c^+ production we take the simple form [16]

$$R_3(x_u, x_d, x_c) = \alpha \frac{x_u x_d x_c}{x_F^2} \delta(x_u + x_d + x_c - x_F), \quad (10)$$

with α fixed by the condition $\int_0^1 dx_F (1/\sigma) d\sigma^{rec}/dx_F = 1$, where σ is the cross section for Λ_c^+ 's inclusively produced in pp collisions. Of course, with this

choice for the parameter α we will not be able to give a prediction for the total cross section for Λ_c^+ production. The recombination model of eq. 7 can only give predictions on cross sections relative to the cross section for a known process. Thus, we could take a different point of view and chose α in order to fit the inclusive x_F distribution for a given reaction, *e.g.* $pp \rightarrow p+X$, and expect that the relative normalizations of the single quark distributions account for the desired proportion of another processes cross sections relative to the $pp \rightarrow p+X$ cross section, as was made in ref. [16]. Instead of it, and since in the case of $pp \rightarrow \Lambda_c^+ + X$ we don't know the total cross section accurately, we simply fix α in order to normalize to 1 the Λ_c^+ 's x_F distribution as given by eq. 7, losing the possibility to give predictions on the total inclusive Λ_c^+ cross section in recombination. Other forms than eq. 10 for the recombination function have been considered in the literature [17, 18, 19]. We have observed that the shape of the inclusive cross section of eq. 7 is practically insensitive to the form of the recombination function as was pointed out in conection with Λ_0 production in pp collisions [16].

Using eqs. 8 and 10 the invariant x_F distribution for Λ_c^+ 's produced inclusively in pp collisions can be written as

$$\frac{2E}{\sqrt{s}\sigma} \frac{d\sigma_{\Lambda_c^+}^{rec}}{dx_F} = \alpha 75 \frac{(1-x_F)^{-0.1}}{x_F^2} \int_0^{x_F} dx_1 F_{u,val}(x_1) \times \int_0^{x_F-x_1} dx_2 F_{d,val}(x_2) F_{c,sea}(x_F-x_1-x_2), \quad (11)$$

where we integrate out over x_3 . The parameter σ is fixed with experimental data.

The inclusive production cross section of the Λ_c^+ is obtained by adding the contribution of recombination (eq. 11) to the QCD processes of eq. 1,

$$\frac{d\sigma^{tot}}{dx_F} = \frac{d\sigma^{pf}}{dx_F} + \frac{d\sigma^{rec}}{dx_F}. \quad (12)$$

The resulting inclusive Λ_c^+ production cross section $d\sigma^{tot}/dx_F$ is plotted in fig. 3 a) and b) using the two fragmentation function of eqs. 5 and 6 and compared with experimental data in pp collisions from the ISR [3]. As we can see, the shape of the experimental data is very well described by our model. We use a factor $\sigma = 0.92(0.72)\mu b$ for Peterson (delta) fragmentation respectively.

Although we are not able to explain the normalization of the ISR data (we need a global factor of 1000 in eq. 12), its x_F dependence is well described by our model.

3 Λ_c^+ production by IC coalescence and fragmentation

In a similar approach R. Vogt *et al.* [7] calculated the Λ_c^+ production in pp and πp collisions. The two component model they use consists of a parton fusion mechanism plus coalescence of the intrinsic charm in the proton.

In ref. [7] it is assumed that Λ_c^+ 's can be produced by coalescence of a c quark with a ud diquark when the coherence of a $|uudc\bar{c}\rangle$ Fock state of the proton breaks due to the inelastic interaction with the target in $pp \rightarrow \Lambda_c^+ + X$ reactions. For Λ_c^+ production in $\pi^- p$ collisions, a $|\bar{u}dc\bar{c}\rangle$ Fock state of the pion is considered.

The frame independent probability distribution of a five particle state of the proton is [7, 8]

$$\frac{dP^{IC}}{dx_u dx_{u'} \dots dx_{\bar{c}}} = N_5 \alpha_s^4 (M_{c\bar{c}}^2) \frac{\delta(1 - \sum_{i=u}^{\bar{c}} x_i)}{(m_p^2 - \sum_{i=u}^{\bar{c}} \hat{m}_i^2 x_i)^2}, \quad (13)$$

with N_5 normalizing the $|uudc\bar{c}\rangle$ state probability.

The intrinsic charm x_F distribution is related to P^{IC} by [7]

$$\begin{aligned} \frac{d\sigma^{IC}}{dx_F} &= \sigma_{pp}^{in} \frac{\mu^2}{4\hat{m}_c^2} \int_0^1 dx_u dx_{u'} dx_d dx_c dx_{\bar{c}} \delta(x_F - x_u - x_d - x_c) \\ &\times \frac{dP^{IC}}{dx_u dx_{u'} \dots dx_{\bar{c}}} \end{aligned} \quad (14)$$

where the factor $\mu^2/4\hat{m}_c^2$ is the result of the soft interaction needed to break the coherence of the Fock state. σ_{pp}^{in} is the inelastic pp cross section.

In ref [7] an attempt is made to fix the soft scale parameter at $\mu^2 \sim 0.2 \text{ GeV}^2$ by the assumption that the diffractive fraction of the total cross section is the same for charmonium and charmed hadrons. In this way they obtain $\sigma_{pN}^{IC} \simeq 0.7 \mu b$ in pN interactions at 200 GeV with $P^{IC} = 0.3\%$.

Since we want to compare the prediction of the IC model for Λ_c^+ production in pp collisions at the ISR energy $\sqrt{s} = 63 \text{ GeV}$, we prefer to fix the unknown product $\sigma_{pp}^{in} \mu^2$ with the experimental data.

The total inclusive cross section for Λ_c^+ production in pp collisions is then given by,

$$\frac{d\sigma^{tot}}{dx_F} = \frac{d\sigma^{pf}}{dx_F} + r \frac{d\sigma_{rec}^{IC}}{dx_F} + \frac{d\sigma_{frag}^{IC}}{dx_F} \quad (15)$$

where r represents the fraction of IC production with respect to parton fusion (see ref. [7]).

The prediction of the IC two-component model is plotted in fig. 3 c) and d) for Peterson and delta fragmentation respectively and compared to the prediction of the recombination two-component model and experimental data from the ISR [3]. We use $\hat{m}_c = 1.8 \text{ GeV}$ as quoted in ref. [7] and $r\sigma_{pp}^{in}\mu^2 = 270(320)$ for delta (Peterson) fragmentation in order to fit the experimental data with the IC two-component model. It must be mentioned that, as with the recombination two-component model, the IC two component-model can not explain the abnormally high normalization of the ISR data and a global factor of 1000 is needed in eq. 15.

4 The Thomas Precession Model and the Λ_c^+ polarization

In the TPM the polarization of hadrons is a consequence of the Thomas precession during the recombination process [9].

A Λ baryon is formed by the recombination of a ud diquark in a spin state $j = m = 0$ and a Q quark originally present in the sea of the projectile, so the spin of the Λ is carried entirely by the Q quark.

Since the recombining quarks in the projectile must carry a fraction of the outgoing hadron's transverse momentum, the Thomas precession appears due to the change in the longitudinal momentum of quarks as they pass from the projectile to the final hadron.

In particular, if the Λ_c^+ is produced through Valence Valence Sea (VVS) recombination, since the x -distribution of sea quarks is very steep, the Λ_c^+ must get most of its momentum from the valence ud diquark. In this case the c sea-quark must be accelerated in passing from the proton sea to the produced Λ_c^+ and the later must be negatively polarized due to the Thomas precession.

On the other hand, if the Λ_c^+ is produced by the coalescence mechanism, since the x -distribution of the intrinsic charm is hard, the Λ_c^+ gets most of its momentum from the intrinsic c -quark, which must be decelerated in the recombination process and consequently the Λ_c^+ is produced with positive polarization [20].

The amplitude for the production of a Λ of spin \vec{s} is proportional to $(\Delta E + \vec{s} \cdot \vec{\omega}_T)$, where ΔE represents the change in energy in going from the quarks to the final state in absence of spin effects and $\vec{\omega}_T \sim \gamma/(1 + \gamma)\vec{F} \times \vec{\beta}$ is the Thomas frequency.

The polarization in the TPM is given by

$$P(p \rightarrow \Lambda) = -\frac{12}{\Delta x M^2} \frac{[1 - 3\xi(x_F)]}{[1 + 3\xi(x_F)]^2} p_{T\Lambda}, \quad (16)$$

where

$$M^2 = \left[\frac{m_D^2 + p_{TD}^2}{1 - \xi(x_F)} + \frac{m_q^2 + p_{Tq}^2}{\xi(x_F)} - m_\Lambda^2 - p_{T\Lambda}^2 \right], \quad (17)$$

where m_D and m_q are the masses and p_{TD} and p_{Tq} the transverse momentums of the ud diquark and c quark respectively, m_Λ and $p_{T\Lambda}$ the mass and transverse momentum of the Λ_c , and $\xi(x_F) = \langle x_Q \rangle / x_F$ the average momentum fraction of the Q quark in the projectile.

To give a quantitative prediction for the polarization, DeGrand and Miettinen take a parametrization for $\xi(x_F)$ and obtain a good description of experimental data [9]. We explicitly compute $\xi(x_F)$ [20, 21] using a recombination model

$$\langle \xi \rangle(x_F) = \frac{\langle x_q \rangle}{x_F} = \frac{\int dx_q x_q \frac{d\sigma}{dx_q dx_F}}{x_F \frac{d\sigma}{dx_F}} \quad (18)$$

where x_F is the Feynman x defined by $x_F = 2p_L/\sqrt{s}$.

The production of $\bar{\Lambda}_c^-$ would have a recombination component which contributes with a smaller fraction to the total cross section. This is a consequence of the fact that in a proton beam the production of the $\bar{\Lambda}_c^-$ takes place through the recombination of sea quarks only.

In the production mechanism via intrinsic charm the $\bar{\Lambda}_c^-$ can only be produced by the c -quark fragmentation in a five particle Fock state. If a nine particle Fock state is considered $|uudc\bar{c}u\bar{u}\bar{d}\bar{d}\rangle$ as pointed out in [11], the x_c distribution would not be as hard as in the five particle Fock state. Therefore the recombination would not decelerate the \bar{c} quark as it happens

with c quark in the Λ_c formation via recombination. Henceforth, the two mechanisms predict zero polarization for the $\overline{\Lambda}_c^-$.

4.1 The polarization in a two component model

The polarization is defined as

$$P(x_F) = \left[\frac{d\sigma_{\uparrow}}{dx_F} - \frac{d\sigma_{\downarrow}}{dx_F} \right] / \frac{d\sigma}{dx_F}, \quad (19)$$

where $d\sigma_{\uparrow}/dx_F$, $d\sigma_{\downarrow}/dx_F$ and $d\sigma/dx_F$ are the spin up, spin down and total cross section respectively. In a scenario where Λ_c^+ s originate in two different processes one must take into account the different contributions to the polarization.

The polarization of baryons in the TPM is the result of the recombination process. Λ_c^+ produced by parton fusion and fragmentation has been shown to have a very small polarization [20] which will be neglected here. We have,

$$\frac{d\sigma^{tot}}{dx_F} = \frac{d\sigma_{\downarrow}^{rec}}{dx_F} + \frac{d\sigma_{\uparrow}^{rec}}{dx_F} + \frac{d\sigma^{pf}}{dx_F}. \quad (20)$$

We now define the fraction of Λ_c^+ produced by parton fusion of the total of Λ_c^+ s produced as

$$g(x_F) = \left[\frac{d\sigma^{pf}}{dx_F} \right] / \left[\frac{d\sigma^{tot}}{dx_F} \right] \quad (21)$$

hence, from eq. 12

$$\frac{d\sigma^{pf}}{dx_F} = \frac{g(x_F)}{1 - g(x_F)} \frac{d\sigma^{rec}}{dx_F}. \quad (22)$$

Using eq. 22 we can rewrite eq. 20 as

$$\frac{d\sigma}{dx_F} = \frac{1}{1 - g(x_F)} \left(\frac{d\sigma_{\downarrow}^{rec}}{dx_F} + \frac{d\sigma_{\uparrow}^{rec}}{dx_F} \right) \quad (23)$$

and with the help of eqs. 20 and 23 we obtain the polarization

$$P(x_F) = [1 - g(x_F)] \left[\frac{d\sigma_{\uparrow}^{rec}}{dx_F} - \frac{d\sigma_{\downarrow}^{rec}}{dx_F} \right] / \left[\frac{d\sigma_{\uparrow}^{rec}}{dx_F} + \frac{d\sigma_{\downarrow}^{rec}}{dx_F} \right] \quad (24)$$

or using eq. 16

$$P(x_F) = - [1 - g(x_F)] \frac{12}{\Delta x M^2} \frac{(1 - 3\xi(x_F))}{(1 + 3\xi(x_F))^2} p_{T\Lambda} \quad (25)$$

where M^2 is given by eq. 17. A similar reasoning gives the same eq. 25 for the polarization of Λ_c^+ produced by intrinsic charm coalescence.

The $g(x_F)$ for the two models are shown in fig. 4.

4.2 The Λ_c^+ polarization

In the coalescence of the intrinsic charm of the proton with quarks in a Fock state the x_F distribution of the Λ_c^+ is given by eq. 14. So that we can write

$$\frac{d\sigma}{dx_c dx_F} = (x_F - x_c) \int_0^{1-x_F} dx_u \left(\frac{x_c(1-x_u-x_F)}{x_c+1-x_u-x_F} \right)^2. \quad (26)$$

If the recombination mechanism occurs among the diquark ud in the proton and the c quark from the proton's sea then, from eq. 11, we have

$$\frac{d\sigma}{dx_c dx_F} = \int_0^{x_F-x_c} dx_u \int_0^{x_F-x_c-x_u} dx_d x_c F_3(x_u, x_d, x_c) R_3(x_u, x_d, x_c). \quad (27)$$

In order to calculate the polarization of the produced Λ_c^+ 's, we need the mean value of $\xi^{IC(rec)}(x_F)$ which is obtained replacing eqs. 26 and 27 into eq. 18 for each case respectively. The $\xi(x_F)$ for these two processes are shown in fig. 5.

We calculate the Λ_c^+ polarization given by eq. 25 for each production mechanism separately using $\xi(x_F)$ as given by eq. 18 with eqs. 27 and 26 for recombination and coalescence respectively.

The Λ_c^+ polarization is plotted in fig. 6 for the two models; parton fusion plus recombination and parton fusion plus IC-coalescence. As in ref. [9] we use $m_D = \frac{2}{3} GeV$, $\langle p_T^2 \rangle_{D,c} = \frac{1}{4} p_{T\Lambda}^2 + \langle k_T^2 \rangle$ with $\langle k_T^2 \rangle = 0.25 GeV^2$ and $\Delta x = 5 GeV^{-1}$. We take $m_c = 1.5 GeV$ and $m_{\Lambda_c^+} = 2.285 GeV$.

5 Conclusions

We studied the Λ_c^+ production in pp collisions in the framework of two component models. We used two different versions of the two component model and compared them. As we can see in fig. 3 c) and d), both versions can describe the shape of the x_F distribution for Λ_c^+ 's produced in pp collisions, but none of them can describe the abnormally high normalization of the ISR data quoted in ref. [3]. At this point it is useful to mention that the normalization of the ISR data has been object of study in other publications (see *e.g.* ref. [22]) and none of them was able to explain it. This discrepancy between theory and experiment does not exist for charmed meson production, which is well described both in shape and normalization with the parton fusion mechanism plus intrinsic charm coalescence [11]. An analysis of charmed meson production using parton fusion and recombination is forthcoming [23].

In pp interactions the intrinsic charm component seems to be consistent with 1% or less of the total charm sea as stressed in ref. [24]. This suggests that the recombination of valence and c -sea quarks may be an alternative mechanism to explain the enhancement in the x_F distribution at large values.

The Thomas Precession Model predicts very different results for the Λ_c^+ polarization in pp collisions for the production mechanisms discussed. Unfortunately, the only known experimental measurement of the Λ_c^+ polarization in pp collisions [4] is not able to give the sign, then we can not obtain definitive conclusions about the production mechanisms of the Λ_c^+ . However, it is interesting to note that the measurement quoted in ref. [4] seems to be compatible with a high value for the Λ_c^+ polarization, despite the large experimental errors, which may indicate that the TPM is not adequate to describe the polarization of hadrons containing heavy quarks. At this respect, it is interesting to note that the TPM predicts small values for the Λ_c^+ polarization because of its big mass, (see eqs. 16 and 17). Moreover, the fact that only a fraction of the total number of Λ_c^+ s produced originated in a recombination process, suppresses the polarization even more.

Another sensible test that can give information about the production mechanisms of hadrons containing heavy quarks is the measurement of hadron anti-hadron production asymmetries. In fact, since the parton fusion mechanism predicts a very small asymmetry at NLO, the asymmetry observed experimentally in charmed hadron production must be produced by conventional recombination or the intrinsic charm coalescence mechanism.

The $\Lambda_c/\bar{\Lambda}_c$ asymmetry has been calculated in pp collisions using the two-component model with intrinsic charm coalescence [7]. In [7], a factor $r = 100$ is needed to describe properly the asymmetry compared to PHYTIA. Such very high value for the parameter r seems unnatural because it produces an enlargement of the intrinsic charm cross section which can not be easily explained. In addition, the intrinsic charm two-component model is not able to describe the shape of the experimentally observed asymmetry in D^\pm production in π^-p interactions [1].

Acknowledgements

J.M and G.H. wish to thank to Centro Brasileiro de Pesquisas Físicas (CBPF), for the hospitality extended to them. We thank H.R. Christiansen for enlightening discussions during the completion of this work.

References

- [1] E791 Collaboration (E.M. Aitala *et al.*), Phys. Lett. **B 371**,157 (1996).
- [2] A.N. Aleev *et al.*, Z. Phys. **C 23**, 333 (1984), G. Bari *et al.*, Nuovo Cimento, **104 A**, 57 (1991).
- [3] P. Chauvat *et al.* Phys. Lett. **B 199**, 304 (1987).
- [4] A.N. Aleev *et al.*, Sov. J. Nucl. Phys. **43**, 395 (1986).
- [5] S.F. Biagi *et al.*, Z. Phys. **C 28**, 175 (1985), G. Bari *et al.*, Nuovo Cimento **104 A**, 787 (1991), R. Werding, WA89 Collaboration, in proceeding of ICHEP94, Glasgow.
- [6] NA3 Collaboration (J. Badier *et al.*), Z. Phys. **C 20**, 101 (1983).
- [7] R. Vogt and S.J. Brodsky, Nucl. Phys. **B 478**, 311 (1996).
- [8] S.J. Brodsky, P. Hoyer, C. Peterson and N. Sakai, Phys. Lett. **B 93**, 451 (1980) and S.J. Brodsky, C. Peterson and N. Sakai, Phys. Rev. **D 23**, 2745 (1981).
- [9] T. De Grand and H. Miettinen, Phys. Rev. **D 23**, 1227 (1981), Phys. Rev. **D 24**, 2419 (1981), T. Fujita and T. Matsuyana, Phys. Rev. **D 38**, 401 (1988) and T. De Grand, *ib.* 403.
- [10] J. Babcock, D. Sivers and S. Wolfram, Phys. Rev. **D 18**, 162 (1978), B.L. Combridge, Nucl. Phys. **B 151**, 429 (1979), P. Nason, S. Dawson and R.K. Ellis, Nucl. Phys. **N 327**, 49 (1989), R.K. Ellis, Fermilab-Conf-89/168-T (1989), I. Inchiliffe, Lectures at the 1989 SLAC Summer Institute, LBL-28468 (1989).
- [11] R. Vogt, S.J. Brodsky and P. Hoyer, Nucl. Phys **B 383**, 643 (1992).
- [12] M. Glück, E. Reya and A. Vogt, Z. Phys. **C 53**, 127 (1992).
- [13] R. Vogt, Z. Phys. **C 71**, 475 (1996).
- [14] C. Peterson, D. Schlatter, J. Schmitt and P. Zerwas, Phys. Rev. **D 27**, 105 (1983).
- [15] K.P. Das and R.C. Hwa, Phys. Lett. **B 68**, 459 (1977).
- [16] J. Ranft, Phys. Rev. **D 18**, 1491 (1978).
- [17] R.C. Hwa, Phys. Rev. **D 22**, 1593 (1980).

- [18] R.C. Hwa, Phys. Rev. **D 51**, 85 (1995).
- [19] E. Takasugi and X. Tata, Phys. Rev. **D 20**, 211 (1979), Phys. Rev. **D 21**, 1838 (1980), Phys. Rev. **D 23**, 2573 (1981), etc.
- [20] L.M. Montaño and G. Herrera, Phys. Lett. **B 381**, 337 (1996).
- [21] G. Herrera, J. Magnin, L.M. Montaño and F.R.A. Simão, Phys. Lett. **B 382**, 201 (1996).
- [22] V.G. Kartvelishvili, A.K. Likhoded and S.R. Slobospitskii, Sov. J. Nucl. Phys. **33**, 434 (1981).
- [23] E. Cuautle, G. Herrera and J. Magnin, in preparation.
- [24] J.J. Aubert *et al.*, Nucl. Phys. **B 213**, 31 (1983) and Phys. Lett. **B 110**, 73 (1983), E. Hoffman and R. Moore, Z. Phys. **C 20**, 71 (1983), B.W. Harris, J. Smith and R. Vogt, Nucl. Phys. **B 461**, 181 (1996).

Figure Captions

Fig. 1: Feynman diagrams involved in the calculation of the LO elementary cross sections of hard processes in parton fusion.

Fig. 2: Recombination picture: a c -quark joins a ud -diquark to build a Λ_c^+ .

Fig. 3: a) x_F distribution predicted by parton fusion with a Peterson fragmentation function (dashed line) and the sum of the QCD and the conventional recombination contributions (solid line).

b) x_F distribution predicted by parton fusion with a delta fragmentation function (dashed line) and the sum of the QCD and the conventional recombination contributions (solid line).

c) x_F distribution predicted by parton fusion plus recombination (full line) and parton fusion plus IC coalescence (dashed line) with the Peterson fragmentation function.

d) Same as in (c) for delta function recombination.

Experimental data (black dots) are taken from ref. 3.

Fig. 4: Fraction $g(x_F)$ of Λ_c^+ produced by parton fusion and conventional recombination (solid line) and IC recombination (dashed line). In (a) the delta and (b) the Peterson fragmentation function was used to describe the hadronization.

Fig. 5: $\xi(x_F)$ obtained from the conventional recombination model (solid line) and from IC coalescence (dashed line).

Fig. 6: Λ_c^+ polarization as a function of x_F at $p_T = 0.5 \text{ GeV}$ for parton fusion plus recombination (lower curves) and parton fusion plus IC coalescence (upper curves):

We show both when a Peterson (solid line) and a delta (dashed line) fragmentation function was used. In a similar way for the upper curves a Peterson (dotted line) and a delta (dot-dashed line) fragmentation function was used in the hadronization.

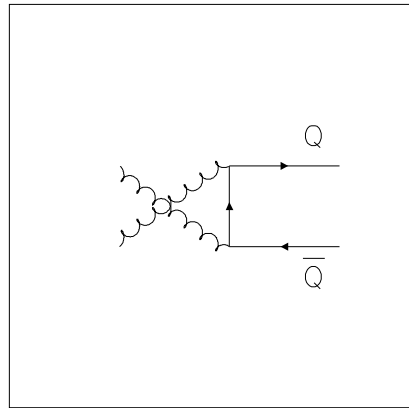
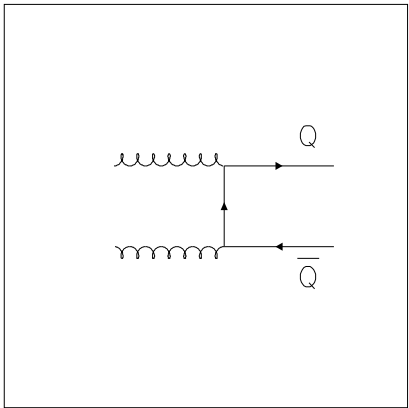
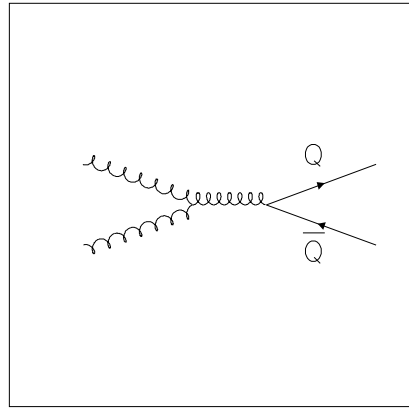
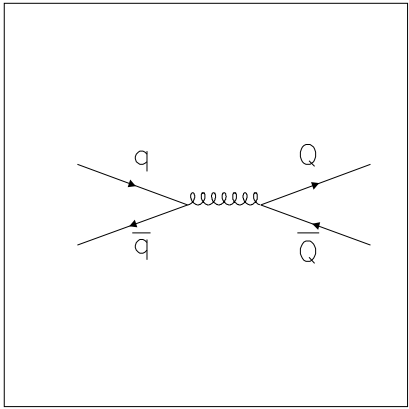


Figure 1:

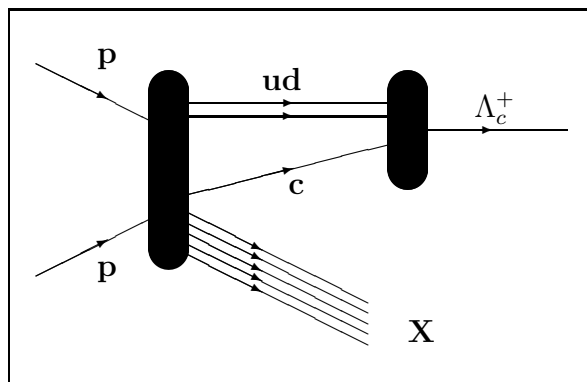


Figure 2:

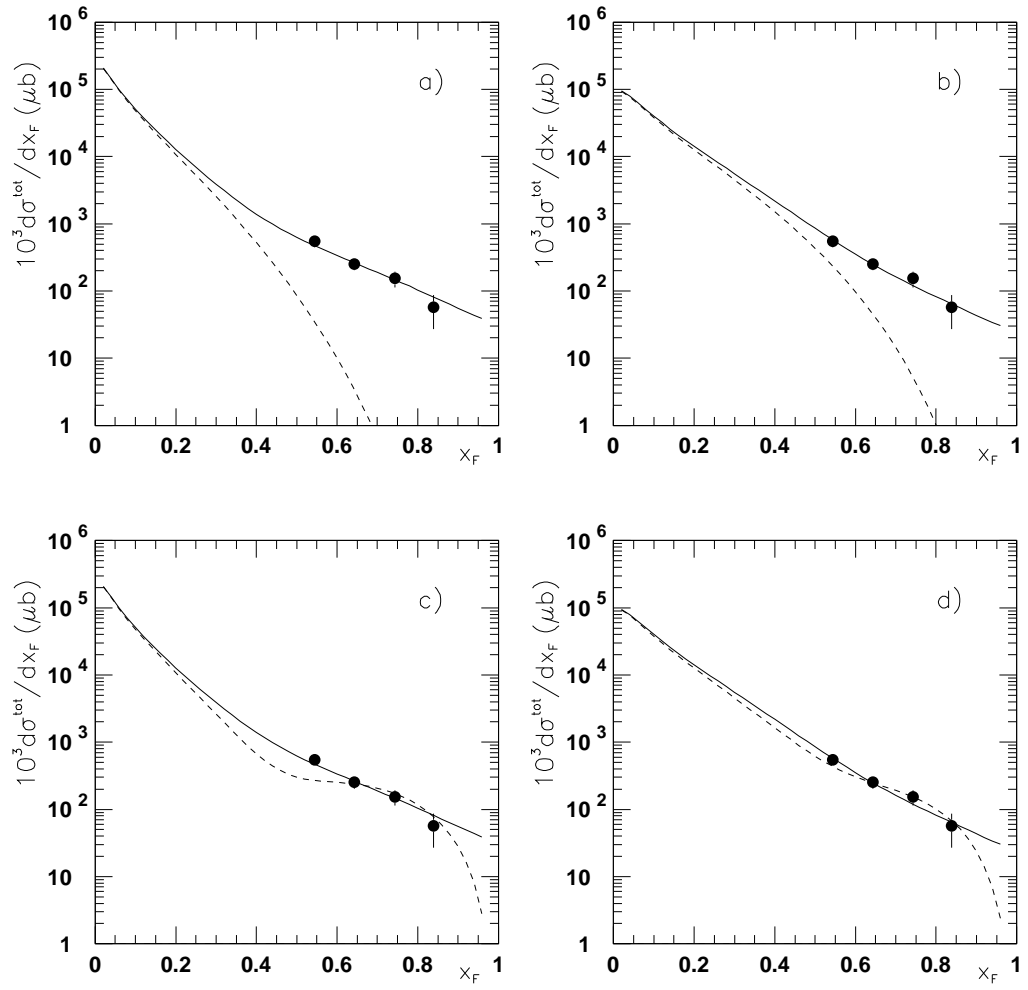


Figure 3:

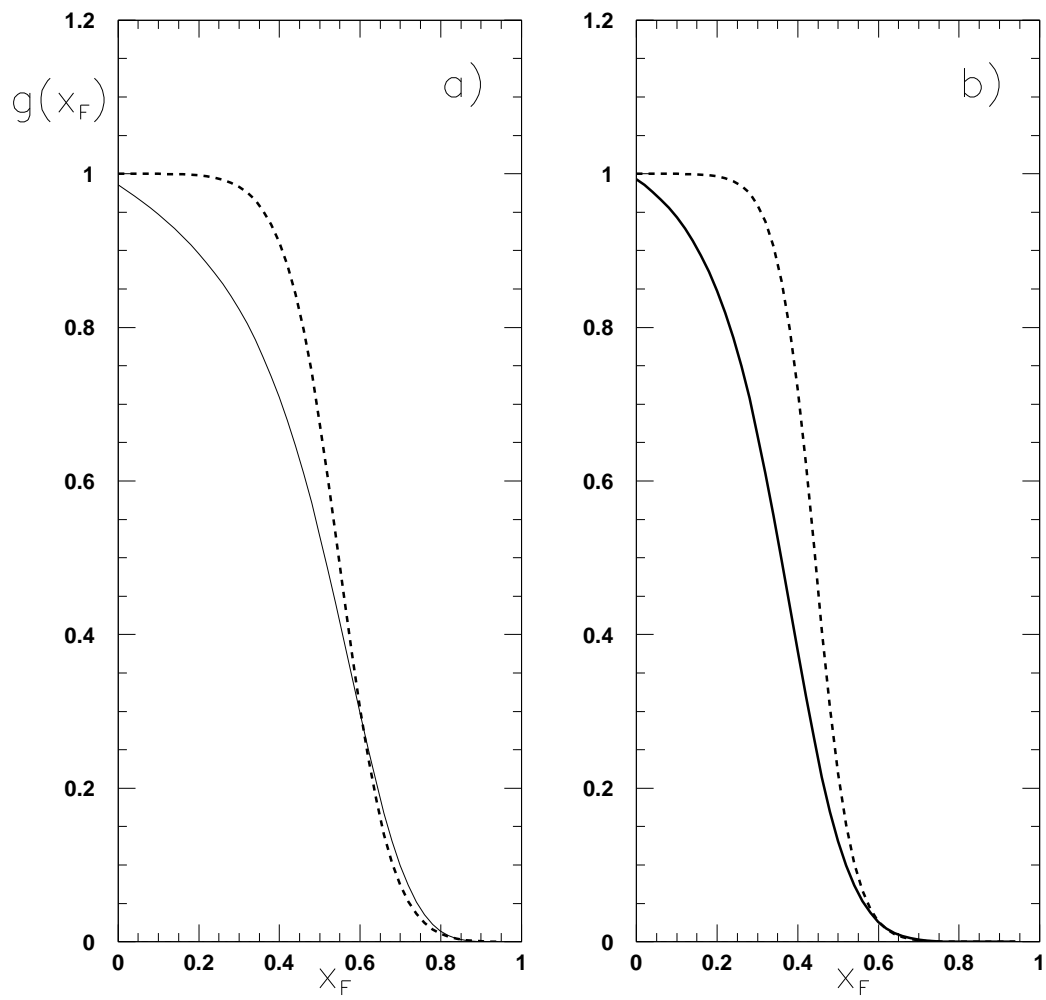


Figure 4:

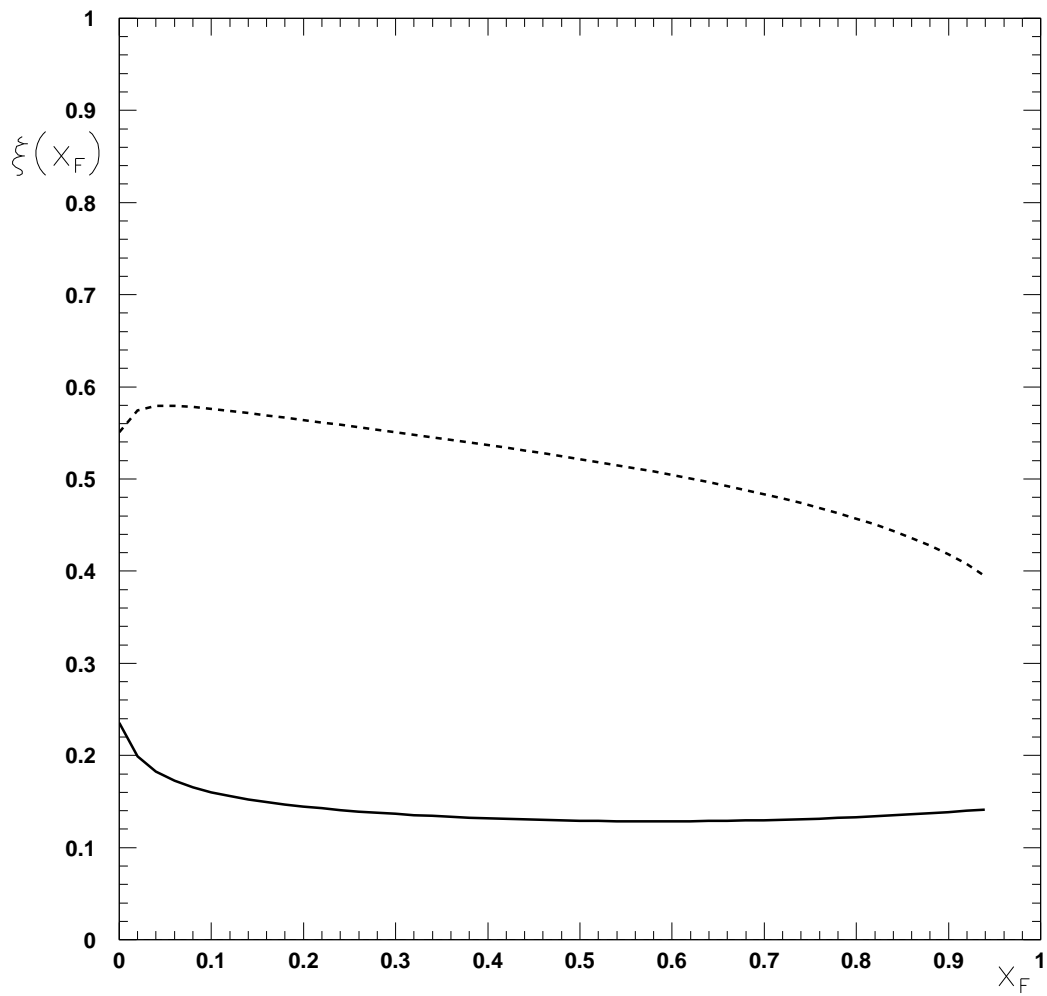


Figure 5:

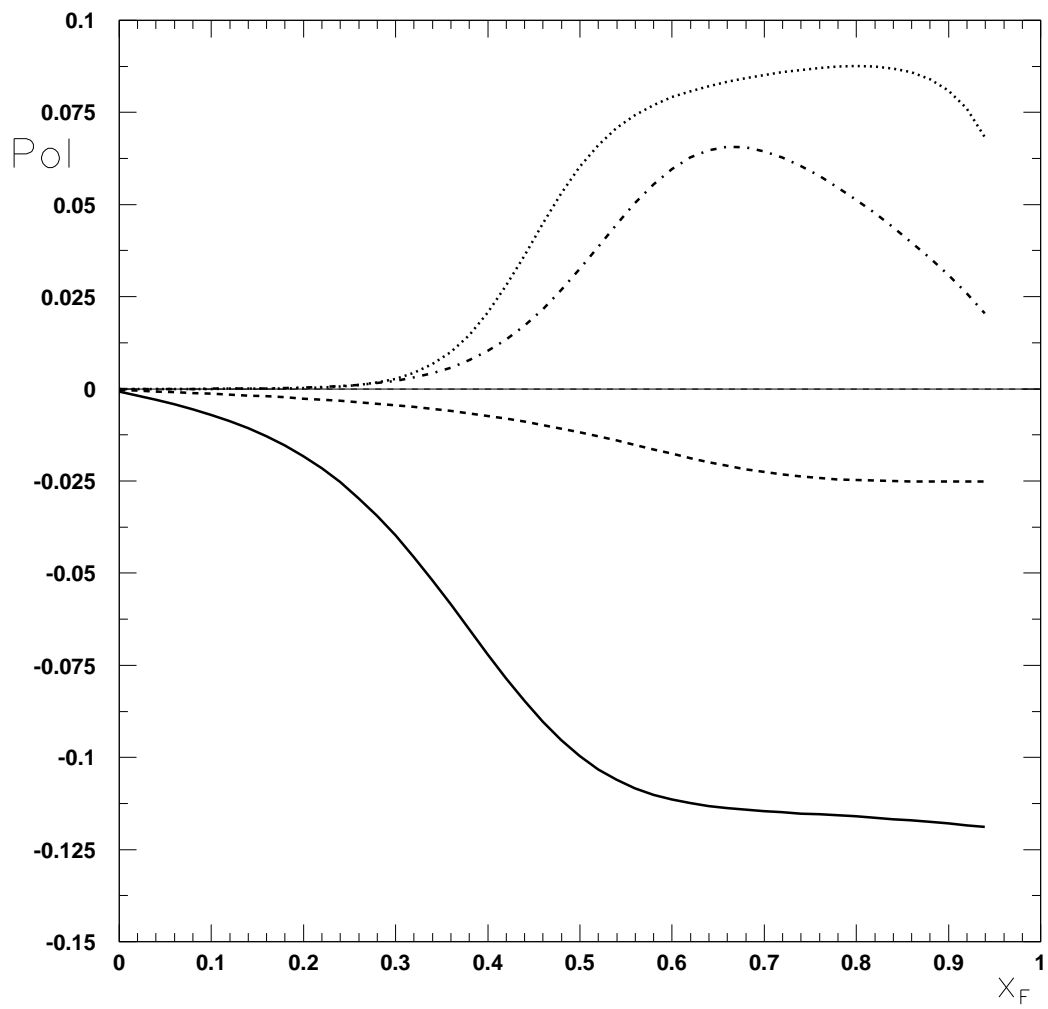


Figure 6: